Supplementary Information

Quantity and accessibility for specific targeting of receptors in tumors

Sajid Hussain[1,2], Maria Rodriguez-Fernandez[3], Gary B. Braun[1,2], Francis J. Doyle III[3] and Erkki Ruoslahti[1,2*]

[1] Cancer Research Center, Sanford-Burnham Medical Research Institute, La Jolla, California 92037, USA

[2] Center for Nanomedicine, and Department of Cell, Molecular and Developmental Biology, University of California Santa Barbara, Santa Barbara, CA 93106-9610, USA

[3] Department of Chemical Engineering, University of California Santa Barbara, Santa Barbara, CA 93106-5080, USA

Supplementary Figures, Tables and Model development details.

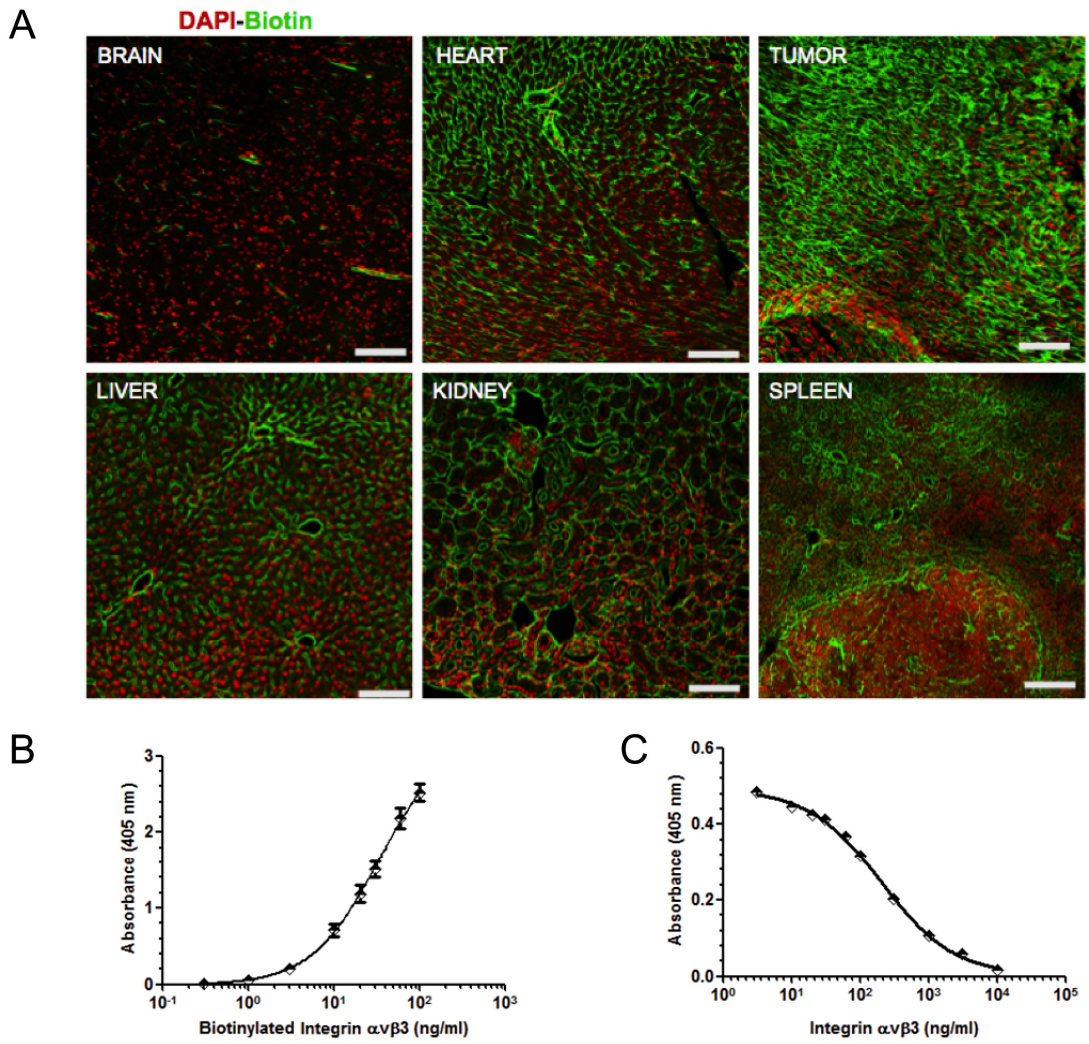

Figure S1. A) Confocal microscopy images of *in vivo* biotinylated tissues and tumor sections from 4T1 tumor bearing mice. Biotin was probed with streptavidin-Alexa Fluor 488 (green), and nuclei were stained with DAPI (red). Representative images of at least five sections from each organs/tumor (n= 4 mice per group; scale bars=100 µm). B, C) The plots of standard curves used for quantifying biotinylated αvβ3 receptors by sandwich ELISA (B) and total receptors by competition ELISA (C).

Mathematical model. The model presented here builds on a published model (1) for antibody uptake and retention in vascularized tumors and captures the major processes that determine the time course of antibody concentration within a tumor including local and systemic clearance, extravasation, diffusion, binding, release, endocytosis, recycling, and degradation. The model equations are:

$$\frac{\partial [Ab]_{free}}{\partial t} = \nabla \cdot \left(D \nabla [Ab]_{free} \right) - \frac{k_{on}}{\varepsilon} [Ab]_{free} [Ag] + k_{off} [Ab]_{bound} \quad (1)$$

$$\frac{\partial [Ab]_{bound}}{\partial t} = \frac{k_{on}}{\varepsilon} [Ab]_{free} [Ag] - k_{off} [Ab]_{bound} - k_e [Ab]_{bound} \quad (2)$$

$$\frac{\partial [Ag]}{\partial t} = R_s - \frac{k_{on}}{\varepsilon} [Ab]_{free} [Ag] + k_{off} [Ab]_{bound} - k_e [Ag] \quad (3)$$

where D is the diffusivity constant, r is the radius, k_{on}, k_{off}, and k_e are the binding, release, and endocytosis rate constants, R_s is the synthesis rate of free antigen, ε is the void fraction, and $[Ab]_{free}$, [Ag], and $[Ab]_{bound}$ are the free antibody, free antigen, and bound antibody/antigen complex concentrations.

We assume that the transport of free antibody to non-vascular tumor cells is governed by the passive diffusion from the tumor vasculature to the different regions of the tumor, plus its concentration changes due to binding and release from the antigen (Eq. 1). Bound antibody similarly changes due to binding and dissociation, and it also decreases due to internalization of the complex (Eq. 2). Finally, free antigen is depleted or restored due to antibody binding and release, and it is also synthesized and internalized (Eq. 3).

At the outer edge of the cylinder we use a no flux or mirror boundary condition:

$$\left. \frac{\partial [Ab]_{free}}{\partial r} \right|_{r=R_{Krogh}} = 0 \quad (4)$$

At the radius of the inner cylinder, we use a mixed boundary condition considering the capillaries as a permeable membrane with permeability P:

$$-\left(\frac{\partial[Ab]_{free}}{\partial r}\right)\Bigg|_{r=R_{Cap}} = \frac{P}{D}\left([Ab]_{plasma} - \frac{[Ab]_{free}}{\varepsilon}\right) \tag{5}$$

The plasma clearance of antibodies is described by a biexponential decay:

$$[Ab]_{plasma}(t) = [Ab]_{plasma,0}\left(Ae^{-k_\alpha t} + Be^{-k_\beta t}\right) \tag{6}$$

where $[Ab]_{plasma,0}$ is the initial plasma concentration, A and B are the fraction of α and β clearance, and k_α and k_β are the clearance rate constants for the α and β phases. This implies the assumption that the dose is large enough that free antigen in the blood and uptake in the tumor do not significantly affect the clearance.

The model parameters used in (1) for a typical high affinity IgG under subsaturating conditions are summarized in Table S1.

Name	Value	Units	Description
$R_{capillary}$	8e-6	[m]	radius of the blood vessels
R_{Krogh}	60e-6	[m]	distance between vessels
E	0.2		effective void fraction
TBV	2e-6	[m^3]	Total Blood Volume
ρ_{tissue}	1e6	[g/m^3]	Tumor density
D	1e-11	[m^2/s]	diffusivity tissue
P	3e-9	[m/s]	permeability vessels
k_{on}	8.6e1	[$mol^{-1}m^3s^{-1}$]	binding rate constant
k_{off}	8.6e-5	[s^{-1}]	release rate constant
K_d	1e-6	[mol/m^3]	dissociation constant
k_e	1.3e-5	[s^{-1}]	endocytosis rate constant
A_{decay}	0.7		fraction of α clearance
B_{decay}	0.3		fraction of β clearance
k_α	log(2)/(1*24*3600)	[s^{-1}]	clearance rate for the α phase
k_β	log(2)/(7*24*3600)	[s^{-1}]	clearance rate for the β phase
Ab_{plasma}	100e-6	[mol/m^3]	Ab initial concentration plasma

Ab_{tissue}	0	[mol/m^3]	Ab initial concentration tissue
Ab_{walls}	0	[mol/m^3]	Ab initial concentration wall vessels
Ag_0	500e-6	[mol/m^3]	Ag antigen initial concentration
Circulation time	14*24*3600	[s]	Circulation time of the Ab

Table S1. Model parameters used in (1)

Thurber et al. (1) consider the concentration of antigen (receptor) to be constant, assuming that $[Ab]_{total}<<[Ag]$. Even if the total amount of antigen in the tumor is larger than the number of antibody molecules, our experimental data suggest that the number of available receptors is much lower than the total number. In order to account for the local decrease in concentration due to binding, we do not assume constant antigen concentration. In contrast, we use Eq. 3 assuming perfect recycling of the antigen ($R_s=k_e[Ag]$):

$$\frac{\partial [Ag]}{\partial t} = -\frac{k_{on}}{\varepsilon}[Ab]_{free}[Ag] + k_{off}[Ab]_{bound} \quad (7)$$

The main advantage of the model at hand is that all of the model rates are physical processes and parameters can be measured with independent experiments, providing insight into which mechanism will improve targeting.

Sensitivity analysis using antibody as drug. To gain insight into the important processes underlying antibody targeting, we performed a relative local sensitivity analysis (2), focusing on a change of the %ID/g at 1 hour when each of the parameters is varied by the same small percentage, using the pre-established model parameters (**Table S1, Figure S2**) (1). The results of sensitivity analysis are as follows: the most important parameter to %ID/g is the radius of the Krogh cylinder (R_{Krogh}) and is directly related to the degree of vascularization in the tumor. A smaller R_{Krogh} indicates less distance between vessels, and consequently a greater number of vessels per unit volume. We verified the importance of R_{Krogh} at short and long circulation times (out to 14 days) in **Figure S3**. The %ID/g was substantially sensitive to the endocytosis constant and the slow plasma clearance (B and k_β) only for long circulation times. The

contribution of endocytosis (k_e) is negligible for 1 h antibody circulation time, the time frame for experiments. Similarly and not unexpected, for 1 h the fast plasma clearance parameter (A) is more important than the slow clearance parameter (B). Notably, a small change on the binding and unbinding constants (k_{on} and k_{off}) do not have significant effect on %ID/g under the experimental conditions, nor does the absolute concentration of antigen in the tissue, that confirms antibody is in sub-saturating conditions. This sensitivity analysis measures %ID/g such that even though the amount of antibody in the tumor is highly influenced by the antibody dose ($Ab_{plasma,0}$),the %ID/g remains practically unchanged.

Using parameter estimation techniques (2), we fitted the model to the experimental data corresponding to the %ID of antibody (Ab) per gram tumor. For 4T1 tumors the optimal value found for R_{Krogh} was 57 μm and for BT474 tumors it was 46 μm. This difference suggests that the degree of vascularization is greater for BT474 than for 4T1 tumor.

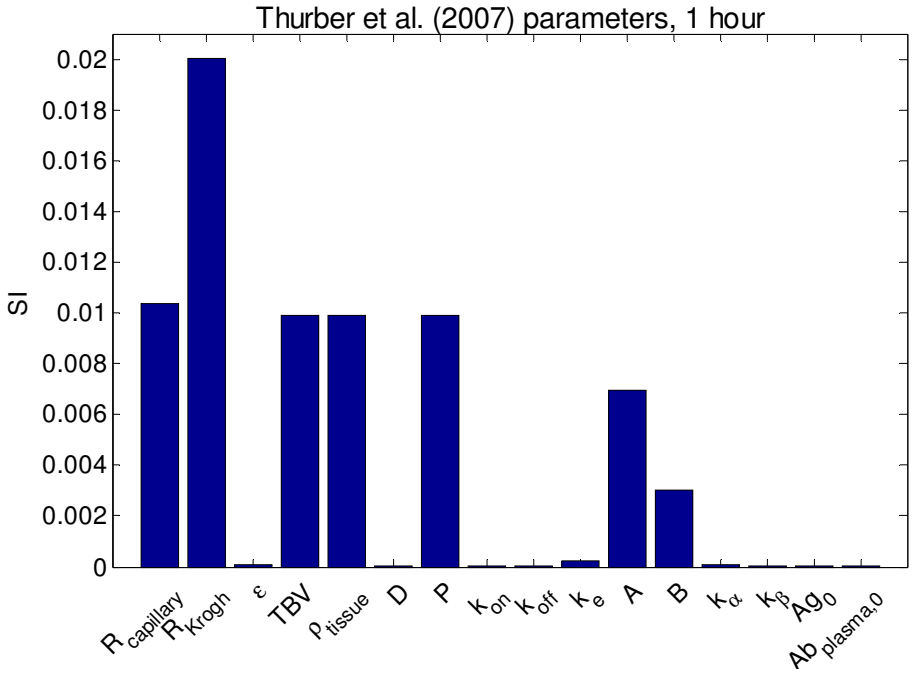

Figure S2. Sensitivity analysis at short circulation times: change of %ID/g after 1 hour of antibody circulation when each of the parameters is varied by the same percentage.

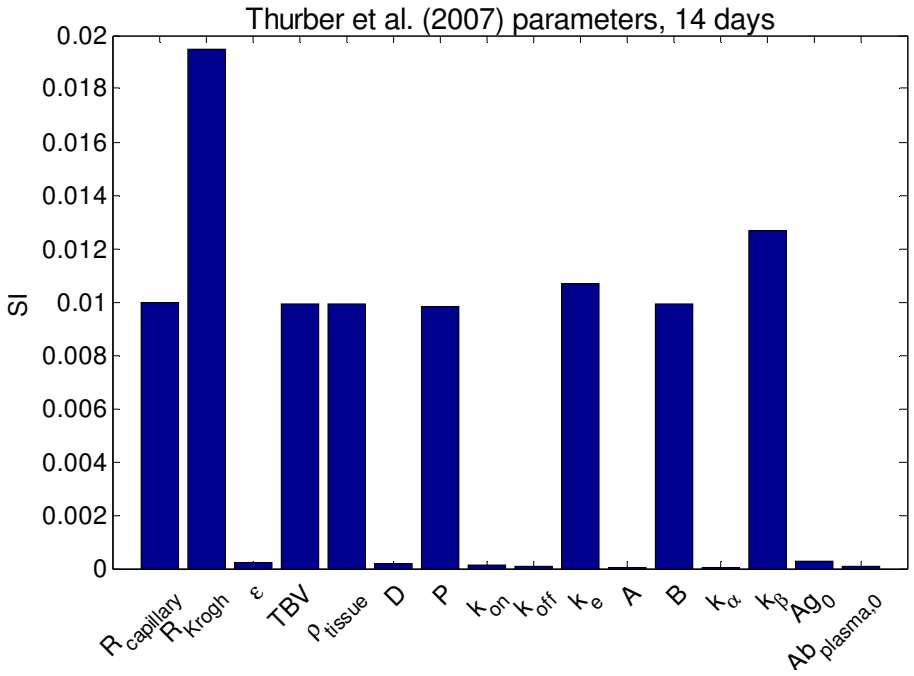

Figure S3. Sensitivity analysis at long circulation times: change of %ID/g after 14 days of antibody circulation when each of the parameters is varied by the same percentage.

Name	4T1/LM609/αvβ3	BT474/Herceptin/HER2	Units
$R_{capillary}$	8e-6	8e-6	[m]
R_{Krogh}	57e-6	46e-6	[m]
E	0.2	0.2	
TBV	2e-6	2e-6	[m^3]
ρ_{tissue}	1e6	1e6	[g/m^3]
D	1e-11	1e-11	[m^2/s]
P	3e-9	3e-9	[m/s]
iRGD-factor	4.5	4.5	[m/s]
k_{on}	8.6e1	71e1	[$mol^{-1} m^3 s^{-1}$]
k_{off}	8.6e-4	3.5e-4	[s^{-1}]
K_d	1e-5	5e-7	[mol/m^3]
k_e	1.3e-5	1.3e-5	[s^{-1}]
A_{decay}	0.7	0.7	
B_{decay}	0.3	0.3	
k_α	log(2)/(1*24*3600)	log(2)/(1*24*3600)	[s^{-1}]
k_β	log(2)/(7*24*3600)	log(2)/(7*24*3600)	[s^{-1}]
Ab_{plasma}	3.3e-4|2e-4	3.4e-4	[mol/m^3]

Ab_{tissue}	0	0	[mol/m^3]
Ab_{walls}	0	0	[mol/m^3]
Ag_0	170e-6	1850e-6	[mol/m^3]
Circulation time	3600	3600	[s]

Table S2. Model parameters used in the simulations.

Biotinylation modeling. Since no information on the value of P or D for the sulfo-NHS-LC-biotin was found in the literature, we estimated these values fitting the model to the biotinylation experimental data with and without iRGD. Sulfo-NHS-LC-Biotin binds to antibodies, proteins and any other primary amine-containing macromolecules. Therefore, for modeling purposes we should not use the concentration of the particular target receptor under study but the total number of molecules to which the biotin can bind. We hypothesize that, for the three tumor types, the concentration of amine-containing molecules is proportional to the total amount of proteins measured with a BCA assay. Moreover, the percentage of accessible proteins, with and without iRGD, can be considered equivalent to the percentage of accessible receptors; therefore, we can compute the expected amount of biotinylated protein. Using this value and, assuming that the ratio between antigen and amine-containing molecule concentration is equivalent to the ratio between antigen and total amount of protein, we calculated the concentration of biotinylated antigen target.

Tumor	iRGD	R_{Krogh} (µm)	P antibody (m/s)	P biotin (m/s)
4T1	**–**	57	3e-9	7.9e-9
4T1	**+**	57	(x4.5) 1.3e-8	(x4.5) 3.6e-8
BT474	**–**	46	3e-9	7.9e-9
BT474	**+**	46	(x4.5) 1.3e-8	(x4.5) 3.6e-8
M21	**–**	38	3e-9	7.9e-9
M21	**+**	38	(x4.5) 1.3e-8	(x4.5) 3.6e-8

Table S3. Fitted permeability values for sulfo-NHS-LC-biotin and injected antibody, with (+) and without (–) iRGD in the three tumor models.

	pmoles/g tumor	No. of molecules/g (x 10^{12})	No. of molecules/cell (x 10^{3})
Human component	31	18.7	18.7
Murine component	4.7	2.8	2.8

Table S4. The fraction of avb3 integrin contributed by host endothelial cells in M21 model is 14% of the total biotinylated avb3 [4.7 / (31+4.7)].

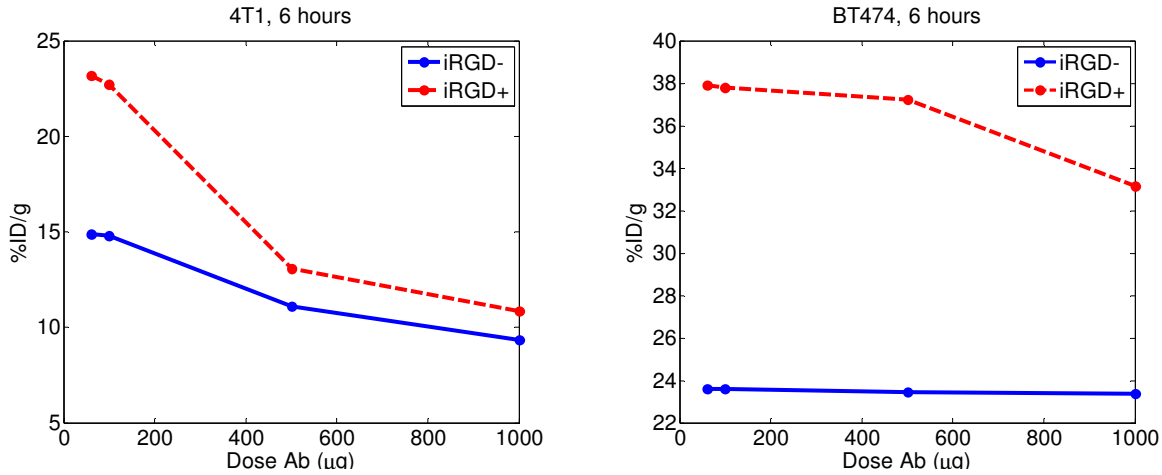

Figure S4. Simulation of 6 hour circulation of the probes with iRGD changing P only during the first hour, and P then returning to the non-iRGD value for the remaining 5 hours. The model still finds a higher %ID/g for both tumors with iRGD. The parameters used for the simulations are summarized in Table S1.

REFERENCES

1. Thurber GM, Zajic SC, Wittrup KD. (2007) Theoretic criteria for antibody penetration into solid tumors and micrometastases. *J Nucl Med*. 48(6):995-9.

2. Rodriguez-Fernandez, M., & Banga, J. R. (2010). SensSB: a software toolbox for the development and sensitivity analysis of systems biology models. *Bioinformatics*, 26(13), 1675-1676.